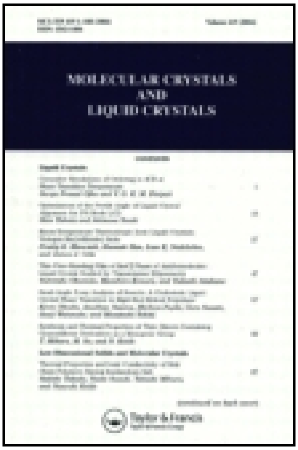

Molecular Crystals and Liquid Crystals
Publication details, including instructions for authors and subscription information:
http://www.tandfonline.com/loi/gmcl20

Improvement of Electro-Optical Characteristics of Liquid Crystal Display by Nanoparticle-Embedded Alignment Layers

Mitsuhiro Akimoto [a], Sudarshan Kundu [a], Koutarou Isomura [a], Itaru Hirayama [a], Shunsuke Kobayashi [a] & Kohki Takatoh [a]
[a] Department of Electronics Engineering and Information Technology, Liquid Crystal Institute, Tokyo University of Science, Yamaguchi, Japan

Version of record first published: 05 Oct 2009

To cite this article: Mitsuhiro Akimoto, Sudarshan Kundu, Koutarou Isomura, Itaru Hirayama, Shunsuke Kobayashi & Kohki Takatoh (2009): Improvement of Electro-Optical Characteristics of Liquid Crystal Display by Nanoparticle-Embedded Alignment Layers, Molecular Crystals and Liquid Crystals, 508:1, 1/[363]-13/[375]

To link to this article: http://dx.doi.org/10.1080/15421400903058130

Mol. Cryst. Liq. Cryst., Vol. 508, pp. 1/[363]–13/[375], 2009

ISSN: 1542-1406 print/1563-5287 online
DOI: 10.1080/15421400903058130

Improvement of Electro-Optical Characteristics of Liquid Crystal Display by Nanoparticle-Embedded Alignment Layers

Mitsuhiro Akimoto, Sudarshan Kundu, Koutarou Isomura, Itaru Hirayama, Shunsuke Kobayashi, and Kohki Takatoh
Department of Electronics Engineering and Information Technology, Liquid Crystal Institute, Tokyo University of Science, Yamaguchi, Japan

The effect of various metal-oxide nanoparticles embedded in the alignment layer of a liquid crystal (LC) display is experimentally investigated. The study mainly focuses on the electro-optical properties of a twisted-nematic LC display. It is confirmed that a certain type of nanoparticles contribute to the enhancement of contrast ratio. In addition, it is observed that for almost all types of nanoparticles used in the present study, the statistical error of electro-optical properties of LC test cells reduces as compared to that of cells without nanoparticles, indicating the improvement of LC molecular alignment. For a further clarification, AFM study and other related measurements are performed.

Keywords: alignment layers; contrast ratio; LCDs; nanoparticles; nematic liquid crystals

1. INTRODUCTION

In recent years, liquid crystal (LC) displays have become ubiquitous in daily life. There are a variety of applications of LC displays including PCs, portable devices and TVs, mainly due to advantages of LC

The authors express their gratitude to Yamaguchi Industrial Promotion Foundation for their support. The authors thanks also to the project 'Cooperation for innovative technology and advanced research in evolutional area (City area),' supported by Ministry of Education, Culture, Sports, Science and Technology (MEXT). The authors are grateful to Nissan Chemical Industries for providing polyimide materials.

Address correspondence to Kohki Takatoh, Department of Electronics Engineering and Information Technology, Tokyo University of Science, Yamaguchai 1-1-1 Daigaku-Dori, San-yo-Onoda, Yamaguchi 756-0884, Japan. E-mail: takatoh@ed.yama.tus.ac.jp

displays such as thin profile, lightweight and low power consumption. Even now, there are strong demands for high-quality LC displays such as low-power consumption, higher response time, and highly qualified production technologies. The fabrication of LC displays and devices requires many technologies, among which well-controlled alignment of LC molecules with desired configuration is quite important. Rubbed polyimide (PI) films have been routinely used to align LC molecules. Thus the characteristics of PI films such as dielectric constant, electrical conductivity determine the quality of LC displays. Much effort has been devoted to providing a better PI by optimizing its chemical structure.

On the other hand, with recent advance of nanotechnology, a variety of metallic and non-metallic nanomaterials such as carbon-based ones (carbon nanotubes, fulleren), nanoparticles and nanorods, are now available to use. Since nanomaterials exhibit size-dependent physical properties in various ways, there is a growing interest in investigating what remarkable properties of nanomaterial itself show, as well as how the addition of nanomaterials into other materials affects physical properties of the host materials. In the field of LC, several research groups have succeeded to improve the performance of LC displays by adding nanoparticles into a LC material [1–4].

In this work, we focus on the use of nanoparticles in PI as a LC alignment layer. Our aim to achieve is twofold. One is the improvement of electro-optical characteristics of LC displays. We already reported that a certain type of nanoparticles added into the PI alignment layer, enhance the contrast ratio remarkably [5]. We again confirmed it in the present study. The second is the improvement of LC molecular alignment, which is suggestive for the production technologies. We found that the statistical error of optical characteristics (here dealing with the contrast ratio only) of LC displays with nanoparticle-embedded alignment layers reduces as compared to ones with the normal alignment layers not containing nanoparticles. It implies that the presence of nanoparticle probably improves the LC molecular alignment at the LC/PI interface. To clarify the effect of nanoparticles on PI, we measured the change in surface morphology, and several other quantities of layer thickness, pretilt angle.

2. EXPERIMENTAL

2.1. Cell Preparation

All nanomaterials used in the present study were supplied as powder by respective suppliers. We restricted ourselves to use only metal-oxide composites of nanomaterials, and employ not only a spherical type of nanomaterial, which includes Barium Titanate, $BaTiO_3$ (BTO) of size 20 nm, 30 nm, 50 nm, 60 nm in diameter (Hereafter we refer to those as BTO-TK20, -TK30, -TK50, -SC60, respectively), MgO (50 nm, referred to as MgO-SX50), $CaCO_3$ (80 nm, 200 nm, referred to as $CaCO_3$-SX80, -SX200, respectively), TiO_2 (23 nm, TiO_2-AL23), but a needlelike-shaped one of TiO_2 (10 by 40 nm, TiO_2-AL10*40). Throughout this study, we refer to these materials as nanoparticles, while only a spherical nanomaterial should be mentioned as nanoparticle in its strict meaning.

First, we prepared a series of dispersions of these nanoparticles at concentrations of 1.0 wt%, 2.0 wt% nanoparticle. As a preliminary, we had tried several solvents into which the powder of nanoparticles are dispersed, and found that γ-Butyrolactone is relatively a good solvent, which is used also for the PI solution. Thus, throughout this study, we used γ-Butyrolactone as a solvent for the dispersions of nanoparticles. Then, each dispersion was added into a standard PI solution, SE-130 (Nissan Chemical Industries, 4.4 wt% PI content), so as to become 2.5 wt% or 5.0 wt% nanoparticles with respect to PI. After stirring and sonicating them enough, each SE-130 solution with nanoparticles was spin-coated onto an ITO glass plate (E.H.C.), and then baked at the temperature and baking time prescribed by the supplier, followed by a short pre-baking. Next, we rubbed ITO glass plates covered with the nanoparticle-embedded alignment layer. A couple of substrates with nanoparticle-embedded alignment layer, as well as ones with neat SE-130 layer, were kept aside for layer thickness measurement and AFM study. The rest were used to fabricate 90 degree twisted-nematic (TN) cells. The cell gap is set at 5 micron by silica spacers (Ube-Nitto Kasei). For reference, TN-LC cells with alignment layers of neat SE-130 were also prepared. All fabrication processes were done in clean-room condition. A well-known nematic LC mixture ZLI-4792 (Merck) was injected into the empty cell by capillary action at the temperature of the isotropic phase, and then the cell was cooled down slowly at the room temperature to stabilize the alignment of the LC molecules.

2.2. V-T Measurements

The voltage versus transmission (V-T) characteristic of the TN-LC cells has been measured using the LC display evaluation system, LCD-5200 of Otsuka Electronics. A square wave voltage of 100 Hz has been applied to switch the liquid crystal molecules and the voltage has been varied from 0 to 10 V.

2.3. AFM Study

The surface topography of the alignment layers has been studied using an atomic force microscope (AFM) instrument, Probe Station model SPI 3700 (SEIKO Instruments). Making use of the bundled software, we can evaluate the surface roughness from the raw data of a surface topography on a PC.

2.4. Thickness Measurement

To measure the thickness of alignment layer, we used the thin film measurement system, F20 of FILMETRICS, which is an optical reflectometer.

2.5. Pretilt Angle Measurement

The pretilt analysis system, PAS-301 (Toyo) is used to measure the pretilt angle of the cells. The apparatus employs the crystal rotation method, which is supposed for an antiparallel-rubbed cell usually, but PAS-301 is optimized for a TN-LC cell as well. Thus we can use the same cells on which the V-T characteristic is to be measured.

3. RESULTS ON THE CONTRAST RATIO

3.1. Enhancement of the Contrast Ratio

We measured the V-T characteristic of each TN-LC cell placed between crossed polarizers at room temperature (25 degree Celsius). This means that the cell works in normally white operation. The transmission is always normalized to unity at no bias voltage. Here, it is worthy to note that any kind of defect due to the addition of nanoparticle was not found in each cell, so that no light leakage and/or light scattering were observed.

Figure 1 shows the result on the contrast ratio from 0 V to 10 V, which is obtained by calculating the V-T data of TN-LC cells. The average value of the test cells is shown in the figure. As one can see from the figure, three types of cells with BTO-embedded alignment layers show higher contrast ratio compared with ones with the neat SE-130 alignment layers. There are other samples exhibiting lower contrast ratio even if they contain BTO nanoparticles. The dependence on concentration is not simple. The other nanoparticles make no positive contribution to the contrast ratio. In addition, all samples do not give any reduction of the threshold voltage. In the case of cells using $CaCO_3$

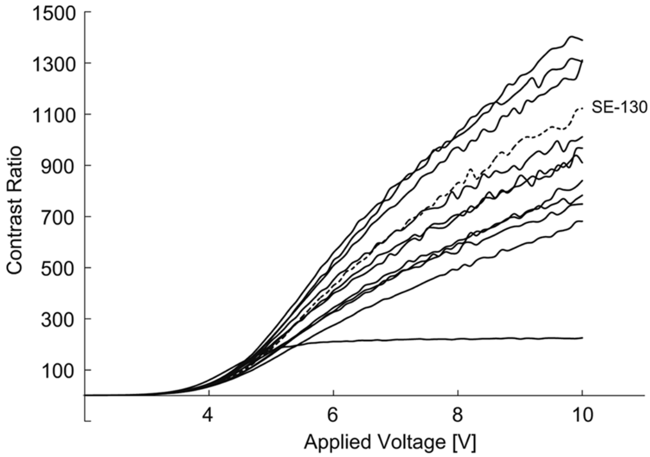

(a)

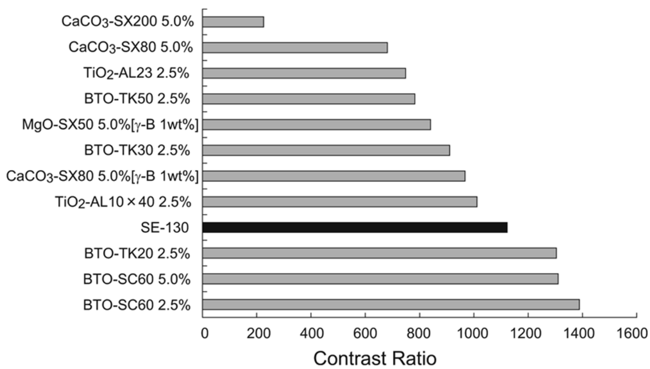

(b)

FIGURE 1 (a) The applied voltage vs. contrast ratio plot. From bottom to top, $CaCO_3$-SX200 5.0% (n = 7), $CaCO_3$-SX80 5.0% (n = 6), TiO_2-AL23 2.5% (n = 7), BTO-TK50 2.5% (n = 4), MgO-SX50 5.0% [γ-B 1.0wt%] (n = 4), BTO-TK30 2.5% (n = 6), $CaCO_3$-SX80 5.0% [γ-B 1.0wt%] (n = 3), TiO_2-AL10*40 2.5% (n = 5), SE130 (n = 6), BTO-TK20 2.5% (n = 15), BTO-SC60 5.0% (n = 19), BTO-SC60 2.5% (n = 23). Here n is the number of sample cells. (b) The variation of contrast ratio at 10 V of applied voltage.

of size 200 nm ($CaCO_3$-SX200), the worst result was obtained; the contrast ratio was saturated at very low value. The fact that a certain type of BTO in the alignment layer enhances the contrast ratio of a TN-LC cell was already reported in our previous study [5]. Here we confirmed the result again.

3.2. Analysis of the Statistical Error

In the Figure 1 of the result on the contrast ratio, only the average values are presented, and the statistical error of the respective line is omitted. From the raw data, we analyzed the statistical distribution of the contrast ratio. In this section, we describe a result on the statistics of the optical characteristics of TN-LC cells.

In addition to the enhancement of the contrast ratio, we found an interesting result of the optical characteristic of TN-LC display employing nanoparticles in the LC alignment layer. That is, the statistical error of the contrast ratio of TN-LC cells with the nanoparticle-embedded alignment layers is reduced remarkably, in comparison with one with the neat SE-130. Almost all nanoparticles including BTOs show the same phenomenon, whether each of them enhances the contrast ratio or not. To express it more quantitatively, we evaluate the improvement rate of the statistical error defined as

$$R = \left(1 - \frac{t_{n-1} \times \frac{\sigma}{\sqrt{n}} \text{ of cells with nanoparticles}}{t_{n-1} \times \frac{\sigma}{\sqrt{n}} \text{ of cells without nanoparticles (SE-130 only)}}\right) \times 100[\%],$$

where σ is the standard deviation of a data set, t_{n-1} is a Student's t-value corresponding to a 95% confidence level and degree of freedom $n-1$ (n corresponds to the number of cells). Student's t-value at a given confidence level is calculated from the cumulative probability of Student's t-distribution, which is usually used to examine the statistics of a given data set for the case when the sample size is small. When the sample size is infinite, Student's t-distribution converges to the normal (Gaussian) distribution, and the associated Student's t-value gives 1.96. The equation $t_{n-1} \times \sigma/\sqrt{n}$ expresses the standard error of data, which yields a 95% confidence interval. If we adopt the data of the cells with the neat SE-130, the improvement rate R must be zero. Therefore a non-zero positive value of R indicates that the standard error of the contrast ratio of cells with nanoparticle-embedded alignment layers reduces; namely, the optical characteristics of TN-LC cells becomes more stable statistically. On the other hand, a negative value of R indicates degradation.

Figure 2 illustrates the explicit values of the improvement rate R. The vertical line of zero percentage corresponds to R of the neat SE-130. As is obvious from the result, the improvement rate exhibits $30\% \sim 80\%$ positive, that means that a considerable reduction of the standard error was observed. In other words, scattering of the result of contrast ratio was narrowed. At 10 V of the bias voltage, the transmission corresponding to a black state takes very low value, so that

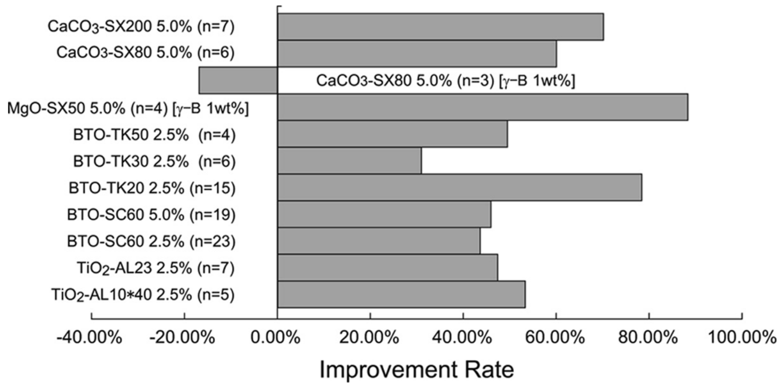

FIGURE 2 Improvement rate of standard errors calculated from the results of contrast ratio at 10 V.

the small change of the transmission causes large difference of the contrast ratio. Therefore, the reduction of standard error of the contrast ratio clearly shows the effect of nanoparticles on the optical characteristic of a LC display. It seems that the reduction of the standard error has no correlation with the enhancement of contrast ratio, since either of BTO nanoparticles marking the higher contrast ratio and other ones resulting degradation, show the same tendency.

4. FURTHER INQUIRIES

The reduction of the standard error mentioned in the previous section, suggests that the presence of nanoparticles probably affects the LC molecule alignment at the interface between LC and PI. To further clarify the phenomenon, we performed several additional measurements, which include the measurement of layer thickness, surface roughness, and pretilt angle.

4.1. Layer Thickness

We measured the thickness of all the nanoparticle-embedded alignment layers with the optical reflectometer. This measurement is necessary to judge the dispersion of nanoparticles into γ-Butyrolactone epared in the first step of the experiment to be at appropriate concentration, since an excess of γ-Butyrolactone used for the solvent works as a thinner for PI solution. Consequently, the thickness of layers using a 2.0 wt% nanoparticle dispersion of γ-Butyrolactone ($\sim$120 nm) is not too much different from one of the neat SE-130 ($\sim$140 nm), while

1.0 wt% nanoparticle dispersion yields thinner layers (~80 nm). It is likely that large difference of thickness affects the eletro-optical characteristic of a TN-LC cell, and thus we will not take into account the results of thinner layers hereafter.

4.2. Surface Morphology

In this subsection, we present the surface morphology of nanoparticle-embedded alignment layers investigated by using AFM. Figure 3 shows a series of AFM images of surface morphology of PI. The surface of the neat SE-130 layer is very flat even though one can see grooves which stem from rubbing, whereas other surfaces have bumps except for the case of $CaCO_3$ nanoparticles of size 200 nm ($CaCO_3$-SX200). Hence it is appropriate to consider that these bumps correspond to nanoparticles. The size of a bump estimated from images, however, is much larger than that of a single nanoparticle, indicating the occurrence of aggregation of nanoparticles in the PI solution. Moreover, the number of bumps does not increase in accordance with the concentration, as we can see from two images of BTO-SC60 at different concentration. This observation also leads to a speculation that the aggregation of nanoparticles occurs in the solution, because a big clump of aggregated nanoparticles should be trapped at the membrane of the syringe filter, when the PI solution was spin-coated. However,

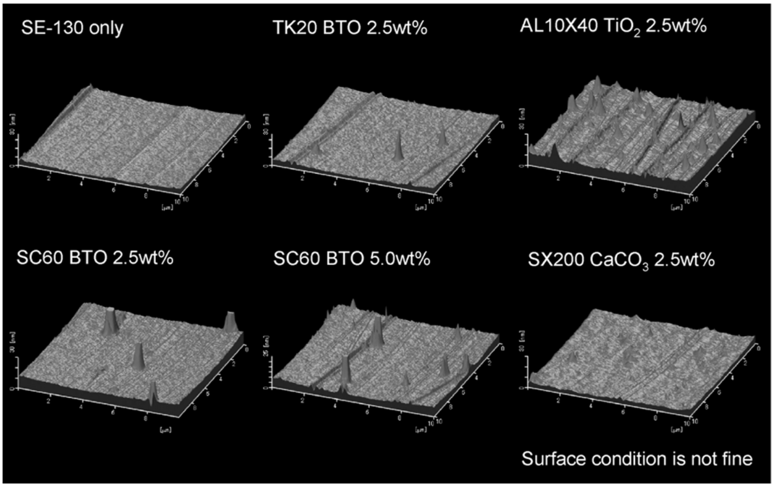

FIGURE 3 AFM images of the surfaces of the rubbed polyimide with nanoparticles.

this is just a subjective impression. We have to discuss it more quantitatively.

Therefore, we evaluated the surface roughness Ra

$$R_a = \frac{1}{L^2} \iint |f(x,y)| dxdy,$$

of each cell by using the bundled software of the AFM instrument. Here the domain of integration in the *xy*-plane is square with side length L, and $f(x, y)$ is the function of vertical distance from the mean plane. As is obvious from Figure 4, every surface roughness of nanoparticle-embedded alignment layer is greater than that of neat SE-130, with the exception of one with $CaCO_3$-SX200. This decrease of surface roughness in the case of $CaCO_3$-SX200, combining the observation of the AFM image of the same cell, brings us to the conclusion that the PI surface with $CaCO_3$-SX200 is too much graveled by nanoparticles or their smashed ones. On the contrary, it might be confusing at first glance that the improvement rate of $CaCO_3$-SX200 shows a higher value as was shown previously, though the contrast ratio itself saturates at a very low value. However, these facts are not inconsistent; since the graveled surface of PI with $CaCO_3$-SX200 nanoparticles probably causes a very averaged light leakage which cannot be detected by visual observation, the transmitted light are also statistically averaged at dark level resulting in the low-value saturation of contrast ratio and the higher improvement rate.

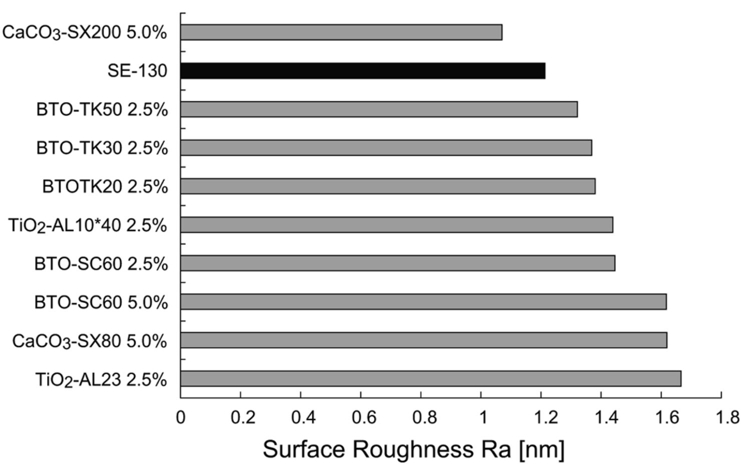

FIGURE 4 Surface roughness of the rubbed polyimide with nanoparticles.

Thus the higher improvement rate of the $CaCO_3$-SX200 case should not be attributed to the improvement of LC molecular alignment. This is a huge degradation of alignment layer and not able to discuss from the viewpoint of LC molecular alignment. Therefore, we omit the result of $CaCO_3$-SX200 in the following discussion.

On the other hand, in case of BTO-SC60, the surface roughness increases linearly with the concentration. This fact seems opposite to the impression obtained above, about possible occurrence of aggregation of nanoparticles, but we do not need to discard that speculation, because the bigger grooves accidentally generated from rubbing also contribute to the increase of surface roughness. Taking into account these facts, we cannot deny the possibility of aggregation of nanoparticles in the PI-nanoparticle solutions.

4.3. Pretilt Angle

Table 1 shows the result of the pretilt angle of TN-LC cells with the nanoparticle-embedded alignment layers and ones with the neat SE-130. The difference between the lowest angle and the highest one is around 1 degree in average, at most 2 degree when including the statistical error. The result of cells with the neat SE-130 lies on the middle. Therefore, a little change of the pretilt angle is generated by the presence of nanoparticles in the PI. BTOs gave the highest three values of the pretilt angle. From these observations, we are inclined to infer that ferroelectricity of BTO nanoparticles contributes the higher pretilt angle. However, it is difficult at present to consider the effect of the dielectric property of nanoparticles on the enhancement of the pretilt angle, because there are other BTOs generating lower pretilt angle.

TABLE 1 The Table of the Pretilt Angles for TN-LC Cells with Nanoparticle-Embedded Alignment Layers

Nanoparticles	Pretilt ($\pm 2\sigma$) [deg.]
TiO_2-AL23 2.5%	2.46 ± 0.59
BTO-TK30 2.5%	2.63 ± 0.62
BTO-TK50 2.5%	2.75 ± 0.67
SE130	2.83 ± 0.46
$CaCO_3$-SX80 5.0%	2.90 ± 0.24
TiO_2-AL10*40 2.5%	3.24 ± 0.41
BTO-TK20 2.5%	3.27 ± 0.33
BTO-SC60 5.0%	3.29 ± 0.28
BTO-SC60 2.5%	3.45 ± 0.41

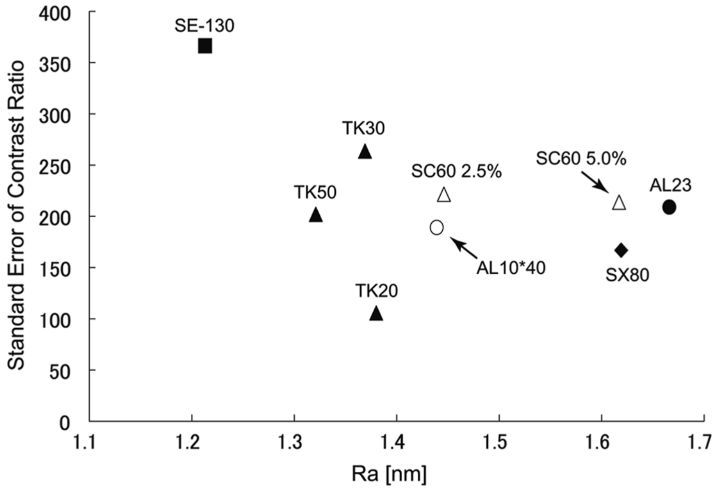

FIGURE 5 The plot of the standard error of contrast ratio against the surface roughness Ra.

4.4. Correlation Between Ra and Others

Next we discuss possible correlation among measured results. Figure 5 shows the data of the standard error of contrast ratio against the surface roughness Ra. Certainly the increase of surface roughness due to the presence of nanoparticles coincides with the reduction of

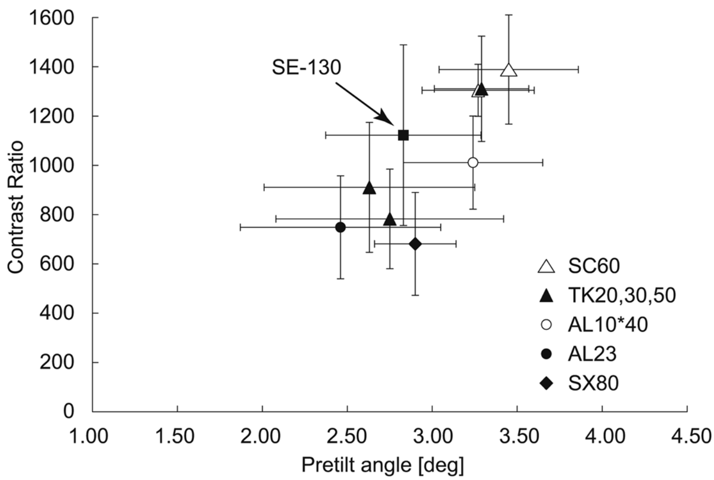

FIGURE 6 The plot of the contrast ratio against the pretilt angle.

the standard error of contrast ratio. However, it seems that there is no strongly positive correlation between the reduction of standard error of contrast ratio and surface roughness of PI with nanoparticles. Namely the larger surface roughness does not necessarily induce the lower value of the standard error of contrast ratio. In Figure 6 contrast ratio is plotted against the pretilt angle. The data of the neat SE-130 is just in the middle, and it is apparent that there is positive correlation between the enhancement of pretilt angle and that of contrast ratio. This correlation is consistent with the fact that BTO nanoparticles embedded in PI of the alignment layer causes slight increase of $\varepsilon_{\parallel}$ while does slight decrease of $\varepsilon_{\perp}$, as presented in our previous study.

5. SUMMARY AND DISCUSSION

In this study, we embedded various nanoparticles into PIs used as the alignment layers of a LC display, and then investigated the effect of nanoparticles on the electro-optical properties of LC display. We confirmed that a certain type of BTO nanoparticles contributes to the enhancement of the contrast ratio, as was reported already by the present authors. In addition, we found that the presence of nanoparticles in alignment layers yields the reduction of statistical error of electro-optical characteristic (contrast ratio) of the TN-LC display, regardless of types of nanoparticles. These results are our achievements to improve the electro-optical characteristics of LC displays by adding various nanoparticles into the alignment layers.

We then performed several additional measurements. AFM observations of surface of PI with nanoparticles revealed that the surface roughness increases in conjunction with the addition of nanoparticles. We showed that there is a correlation between the pretilt angle and the enhancement of contrast ratio, while we could give only an indication that there is a coincidence between the increase of the surface roughness and the statistical stability of optical characteristics of TN-LC cells with nanoparticle-embedded alignment layers.

The increase of surface roughness by nanoparticles means the expansion of the surface area of a PI layer. It is unlikely that nanoparticles embedded are bared on the surface; instead covered with a very thin PI layer. Thus after rubbing the alignment layer, an anisotropic PI is generated even on the surface of (an aggregation) of nanoparticles, which is able to align LC molecules. Hence the reduction of statistical error of electro-optical characteristics probably can be related to the expansion of surface area.

There still remain a lot of matters to be addressed. Further studies should be done to clarify the reason why only a certain kind of BTO is able to enhance the contrast ratio. As is discussed in Ref. [5], ferroelectricity of BTO probably plays an important role. However, we did not observe a direct evidence of ferroelectricity, for example, some kind of hysteresis behavior. We need to check it. One of the other important matters to be concerned is the anchoring strength. It is plausible that the anchoring strength is changed due to the presence of nanoparticle in the PI. These lines of study are now undergoing.

REFERENCES

[1] Reznikov, Y., Buchnev, O., Tereshchenko, O., Reshetnyak, V., Glushchenko, A., & West, J. (2003). *Appl. Phys. Lett.*, *82*, 1917–1919.
[2] Tsai, T.-Y., Huang, Y.-P., Chen, H.-Y., Lee, Wei. L., Chang, Y.-M., & Chin, W.-K. (2005). *Nanotechnology*, *16*, 1053–1057.
[3] Haraguchi, F., Inoue, K., Toshima, N., Takatoh, K., & Kobayashi, S. (2007). *Jpn. J. Appl. Phys.*, *46*, 796–797.
[4] For a review: Qi, H. & Hegmann, T. (2008). *J. Mater. Chem.*, *18*, 3288–3294.
[5] Kundu, S., Akimoto, M., Hirayama, I., Inoue, M., Kobayashi, S., & Takatoh, K. (2008). *Jpn. J. Appl. Phys.*, *47*, 4751–4754.